Robotica (2010) volume 28, pp. 1033–1043. © Cambridge University Press 2010
doi:10.1017/S0263574709990890

A linear optimal tracker designed for omnidirectional vehicle dynamics linearized based on kinematic equations

Kuo-Yang Tu*

Institute of System Information and Control, National Kaohsiung First University of Science and Technology, 2, Juoyue Rd., Nantsu, Kaohsiung 811, Taiwan, R. O. C.

(Received in Final Form: December 14, 2009. First published online: January 15, 2010)

SUMMARY

It is difficult to design controllers for the complicated dynamics of omnidirectional vehicles steered by multiple wheels with distributed traction force. In this paper, the dynamic model of a three-wheel omnidirectional vehicle, which is linearized to simplify controller design, is developed. The conditions of making its dynamics linear are derived first. Then, a strategy of planning wheel velocities to satisfy these conditions is proposed. Consequently, three-wheel omnidirectional vehicle can be easily treated by classical linear control theories. Finally, a linear optimal tracker is designed to control the omnidirectional vehicle for desired movement trajectories. In particular, the dynamic model includes the motors installed in the three-wheel omnidirectional vehicle, making it a practical model. Three kinds of vehicle trajectories illustrate the planning of wheel trajectories for linearizing the vehicle dynamics, and simulations demonstrate the performance of the linear optimal tracker. In addition, experimental results of a practical three-wheel omnidirectional vehicle are also included.

KEYWORDS: Omnidirectional vehicles; Vehicle dynamics; Vehicle control; Kinematic constraint; Optimal tracking control; Tracking control; Trajectory planning.

1. Introduction

The high maneuverability of omnidirectional vehicles makes movement fast and easy in tight spaces,[22] and that has prompted researchers to develop popular mobile robots.[20] That is the reason why the small-size and middle-size leagues of RoboCup, a competition in which teams of autonomous robots play soccer,[5] make frequent use of omnidirectional vehicles. There has been tremendous research interest in omnidirectional vehicles in the recent years.[3,4]

Omnidirectional vehicles are steered by at least three traction force generated by the wheels. In this way any combination of linear and rotational acceleration can be achieved independently of the current orientation of the robot.[8] This is different from traditional three-wheel mobile robot where, under nonholonomic constraint, one wheel guides its direction and the other two control the velocity.[6] A microrobot, 8 mm in length, 6 mm in width and 6 mm in height, is implemented in ref. [19]. The accuracy of kinematics has become important in the research and development of omnidirectional mobile robots, as investigated in ref. [13–14]. The combined force guided by the complicated interaction among three omnidirectional wheels improves the vehicle mobility, but makes dynamics complicated.[2] For accurate dynamic equations, Balakrishna and Ashitava[1] modeled single-wheeled slip, and, in a further development, William, II *et al.*[25] modeled multi-wheeled slip for controller design.

Since omnidirectional vehicles are in general designed by the degree of freedom of motion more than workspace dimensions, how to generate an effective trajectory becomes a vital issue. Muñoz *et al.*[21] connected waypoints to generate a path by using a sequence of splines. Because the splines contained time information, the desired velocity of vehicles could be limited by considering the hardware used. Faiz and Agrawal[7] approximated the set of all feasible states of the system with a set of linear inequalities, which involved the dynamics and other constraints. Huang and Tsai[15] proposed a controller for simultaneous tracking and stabilization in polar coordinates. Moore and Flann[20] presented a trajectory generation algorithm based on an A^* algorithm for an off-road vehicle. The path generator searched for a path achieving a set of vehicle mission goals. In addition, trajectory generation based on optimal strategies is more useful for vehicle performance. For example, according to time-optimal rules, the generated trajectory is solved for the shortest time to arrive at a target location. In this situation, it is necessary to check for a consistent coupling between low-level control and motion planning.[11] Kalmá-Nagy *et al.*[17] employed time optimality to derive the minimum time trajectory for real-time computation in dynamic environment. Similarly, Purwin and D'Andrea[23] implemented an algorithm for four-wheeled omnidirectional vehicles. In this paper, an easier way to control a three-wheel omnidirectional vehicle based on linearizing dynamics is proposed. In contrast to minimum time trajectories developed by Kalmár-Nagy *et al.*[17] and Purwin and D'Andrea,[23] the wheels' velocity trajectories that lead an omnidirectional vehicle dynamics to be linear are derived. As its dynamics is linear, controlling an omnidirectional vehicle to follow a desired trajectory becomes easy.

Kinematic equations of a vehicle involve the velocity relationship between wheels and body. Vehicle dynamics influences its body movement, but the traction force of the vehicle results from the wheels' rotation, which in turn is

* Corresponding author. E-mail: tuky@ccms.nkfust.edu.tw

related to its body movement via kinematics. Intuitively, kinematics relates to dynamics when a vehicle is steered by wheels' traction force. In this paper, a dynamic model simplified by kinematic constraints is proposed. Although many researchers have developed control algorithms based on back-stepping design to combine kinematics into dynamics,[9,12,16] their ideas focused almost exclusively on vehicle dynamics in their control models. The aim of this research is to develop a simplified model based on vehicle dynamics combined with its kinematics for easy controller design. In fact, the complicated dynamics of a three-wheel omnidirectional vehicle solved by kinematics becomes a simple linear model. A linear optimal tracker is thus suitable for the difficult problem of controlling the three-wheel omnidirectional vehicle. The kinematics involved in the dynamics of the three-wheel omnidirectional vehicle simplifies its control problem. That is the main contribution of this paper.

The kinematic transformation of wheel velocity to the velocity of the three-wheel omnidirectional vehicle is the vital factor in linearizing its dynamics. The control problem of the three-wheel omnidirectional vehicle turns into a problem of planning wheel velocity trajectories to maintain linear dynamics. In this paper, three cases used as examples illustrate the problem of planning wheel trajectories for linear dynamics. In addition, a linear optimal tracker solves the control problem of the three-wheel omnidirectional vehicle in linear dynamics. This research demonstrates that the hard problem of controlling the three-wheel omnidirectional vehicle becomes easy trajectory planning rather than complicated dynamics.

The remainder of this paper is organized as follows. In Section 2, new nonlinear dynamic equations of a three-wheel omnidirectional vehicle including motor model are derived. The conditions of making the new nonlinear dynamic equations linear are derived in Section 3. In Section 4, a linear optimal tracker for easily controlling the three-wheel omnidirectional vehicle is proposed. A way to plan wheels' velocity trajectories to maintain the conditions of the vehicle in linear dynamics is proposed in Section 5. In Section 6, the designed controller is demonstrated by simulation and experiments. Finally, conclusions and discussion are given in Section 7.

2. Preliminaries

In this section, the kinematics and dynamics of a three-wheel omnidirectional vehicle are reviewed to figure out its control difficulties. The dynamics of the omnidirectional vehicle derived in the study is an exact model, including motors. The relationship between motor traction force and vehicle motion is also included.

Figure 1 is a kinematic model of a three-wheel omnidirectional vehicle, where (x_b, y_b) is the workspace frame, (x_r, y_r) is the vehicle frame, 1–3 are three wheels, and D_1–D_3 are the unit vectors at the traction direction steered by the three wheels. Let

$$R(\theta) = \begin{bmatrix} \cos\theta & -\sin\theta \\ \sin\theta & \cos\theta \end{bmatrix} \tag{1}$$

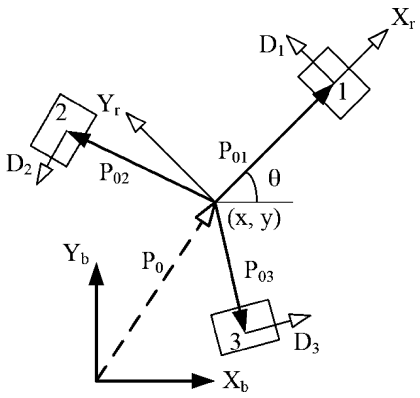

Fig. 1. Geometry of a three-wheel omnidirectional vehicle.

be the transformation of a vector rotated with counterclockwise angle θ. Then, the wheels' position vectors can be easily represented with respect to (x_r, y_r) as follows:

$$P_{01} = L\begin{bmatrix} 1 \\ 0 \end{bmatrix},\ P_{02} = R\left(\frac{2\pi}{3}\right)P_{01} = \frac{L}{2}\begin{bmatrix} -1 \\ \sqrt{3} \end{bmatrix},$$
$$P_{03} = R\left(\frac{4\pi}{3}\right)P_{01} = -\frac{L}{2}\begin{bmatrix} 1 \\ \sqrt{3} \end{bmatrix}, \tag{2}$$

where L is the distance between the wheels' drive points and the center of mass (CM) of the vehicle. In addition, the unit vectors D_i, of the wheel rolling direction, are given by

$$D_i = \frac{1}{L}R\left(\frac{\pi}{2}\right)P_{0i}, \quad \text{that is, } D_1 = \begin{bmatrix} 0 \\ 1 \end{bmatrix},$$
$$D_2 = -\frac{1}{2}\begin{bmatrix} \sqrt{3} \\ 1 \end{bmatrix},\ D_3 = \frac{1}{2}\begin{bmatrix} \sqrt{3} \\ -1 \end{bmatrix}. \tag{3}$$

It is convenient to calculate absolute position and velocity as the vehicle is moving by transforming the vehicle frame (x_r, y_r) to workspace frame (x_b, y_b). Let the vector $P_0 = [x, y]^T$ be the position of the CM in the workspace frame. Then, the drive positions and velocities of three wheels are given by

$$\mathrm{r}_i = P_0 + R(\theta)P_{0i}, \tag{4}$$

$$\mathrm{v}_i = \dot{P}_0 + \dot{R}(\theta)P_{0i}, \text{ respectively}, \quad \text{for } i = 1, \ldots, 3. \tag{5}$$

And then the individual wheel velocities are

$$v_i = v_i^T(R(\theta)D_i). \tag{6}$$

Substituting Eq. (5) into Eq. (6) results in

$$v_i = \dot{P}_0^T R(\theta)D_i + P_{0i}^T \dot{R}^T(\theta)R(\theta)D_i. \tag{7}$$

Let $V = [v_1\ v_2\ v_3]^T$ be the wheels' velocity vector, and $X = [x\ y\ \theta]^T$ be the vehicle configuration vector. Then, their relationship satisfies[17]

$$V = P(\theta)\dot{X} \tag{8}$$

https://doi.org/10.1017/S0263574709990890 Published online by Cambridge University Press

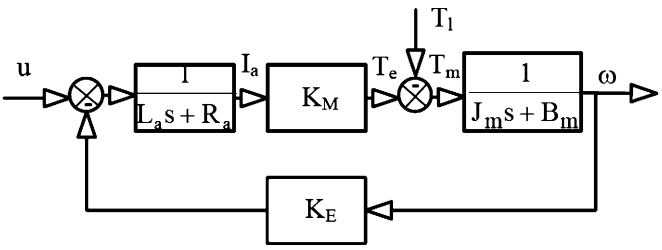

Fig. 2. A motor model.

with

$$P(\theta) = \begin{bmatrix} -\sin\theta & \cos(\theta) & L \\ -\sin\left(\frac{\pi}{3}-\theta\right) & -\cos\left(\frac{\pi}{3}-\theta\right) & L \\ \sin\left(\frac{\pi}{3}+\theta\right) & -\cos\left(\frac{\pi}{3}+\theta\right) & L \end{bmatrix}.$$

Equation (8) is usually named the inverse kinematics equation of the three-wheel omnidirectional vehicle. The motor traction force is the source of the vehicle motion.

A model of the vehicle motor is depicted by Fig. 2, where T_l is the torque of a rolling vehicle wheel, $T_m = (J_m s + B_m)\omega$ is the steering torque of the motor rotor. Notice that J_m and B_m are the inertia moment and the viscous friction of the motor rotor, respectively. If the motor steers via a gear box, B_m includes gear viscous friction. As shown in Fig. 2, the torque of a rolling wheel is

$$T_l = K_M \frac{u - K_E\omega}{R_a + L_a s} - (J_m s + B_m)\omega \tag{9}$$

where ω is the angle velocity of the motor, R_a is armature resistance, L_a is armature inductance, K_M is a torque constant, K_E is the back-EMF (electromotive force) constant, and u is the driving source of the motor.

It is crucial to understand the relationship between motor traction force and vehicle motion to calculate the dynamics of the three-wheel omnidirectional vehicle. The following Lemma derives this relationship.

Lemma 1: Let f be the motor traction force, u be the driving source of the motor, v be the linear velocity from the rolling motor, and n is the gear ratio of the motor. If T_l is constant, then the motor traction force can be approached by

$$f = \alpha u - \beta v + d(\omega), \tag{10}$$

where

$$\alpha = \frac{K_M}{R_a r}, \beta = \frac{nK_M K_E}{R_a r^2} + \frac{nB_m}{r^2},$$

and

$$d(\omega) = -\left[\frac{J_m L_a}{R_a r}\ddot{\omega} + \left(\frac{J_m}{r} + \frac{B_m L_a}{R_a r}\right)\dot{\omega}\right].$$

Proof. From Eq. (9), the torque equation becomes

$$R_a T_l + L_a s T_l = K_M(u - K_E\omega) - (J_m s + B_m)(L_a s + R_a)\omega. \tag{11}$$

Constant T_l makes $L_a s T_l$ into a trivial term. Then, Eq. (11) can be reduced as

$$R_a T_l = K_M(u - K_E\omega) - (J_m s + B_m)(L_a s + R_a)\omega. \tag{12}$$

In a motor, the linear and angular velocities have the following relationship:

$$\omega = nv/r, \tag{13}$$

where n is the gear ratio of the motors, and r is the wheel radius. Substituting Eq. (13) into Eq. (12) and manipulating results in the traction force as follows,

$$f = \frac{T_l}{r} = \frac{K_M}{R_a r}u - \left(\frac{nK_M K_E}{R_a r^2} + \frac{nB_m}{r^2}\right)v - \left[\frac{J_m L_a}{R_a r}\ddot{\omega} + \left(\frac{J_m}{r} + \frac{B_m L_a}{R_a r}\right)\dot{\omega}\right].$$

□

The meaning of Eq. (10) is the motor traction force related to its driving source u, and linear velocity v. The equation holds, as T_l is constant. Generally, the condition of constant T_l happens as the wheel is steered on uniform floor at a constant velocity. If the wheel accelerates or decelerates, the condition is violated, making the traction force of the motor more complicated. In order to alleviate this influence, the motion planning cannot use overly large accelerations or decelerations. In addition, the term $d(\omega)$ is related to angular acceleration and $\ddot{\omega}$ (jerk) is the high-order term of motor angular velocity. Like the most methods of modeling, the high-order term of motor velocity $d(\omega)$ can be neglected for a simple model and regarded as the disturbance in the controller design. In Section 5, alleviating the influence of the disturbance $d(\omega)$ will be solved by trajectory planning. Assume that the vehicle movement results solely from the traction force of its three wheels without slip. The traction force results in linear and angle momentum as follows:

$$\sum_{i=1}^{3} f_i\, R(\theta) D_i = m\ddot{P}_0, \tag{14}$$

$$L\sum_{i=1}^{3} f_i = J\ddot{\theta}, \tag{15}$$

where f_i is the magnitude of the traction force produced by the ith motor, the unit vector D_i is the unit vector of rolling direction of the ith wheel, m is the mass of the vehicle, and J is its inertia moment. Substituting Eq. (10) into Eqs. (14)

https://doi.org/10.1017/S0263574709990890 Published online by Cambridge University Press

and (15) results in the following differential equation:

$$\begin{bmatrix} m\ddot{x} \\ m\ddot{y} \\ J\ddot{\theta} \end{bmatrix} = \alpha \hat{P}(\theta)U(t) - \frac{3\beta}{2}\begin{bmatrix} \dot{x} \\ \dot{y} \\ 2L^2\dot{\theta} \end{bmatrix} + \hat{P}(\theta)D(t) \quad (16)$$

with

$$\hat{P}(\theta) = \begin{bmatrix} -\sin\theta & -\sin\left(\frac{\pi}{3}-\theta\right) & \sin\left(\frac{\pi}{3}+\theta\right) \\ \cos\theta & -\cos\left(\frac{\pi}{3}-\theta\right) & -\cos\left(\frac{\pi}{3}+\theta\right) \\ L & L & L \end{bmatrix},$$

$$U(t) = \begin{bmatrix} u_1(t) \\ u_2(t) \\ u_3(t) \end{bmatrix}, \quad \text{and } D(t) = \begin{bmatrix} d(\omega_1) \\ d(\omega_2) \\ d(\omega_3) \end{bmatrix}.$$

It is difficult to design a controller for the nonlinear and time-varying dynamic system as Eq. (16). Simplifying this dynamics for easy control of three-wheel omnidirectional vehicles was a major motivation of this study. The methods to do so are presented in the following sections.

3. The Dynamics of Omnidirectional Vehicles Simplified by Its Kinematics

The main idea of this paper is to simplify the dynamics of the three-wheel omnidirectional vehicle as a linear time invariant model. In this section, the conditions of the vehicle in a simplified model are derived. The usage of these conditions is also discussed.

The main idea of simplifying the vehicle model is to combine its kinematics into its dynamics. The vehicle forward kinematic equation derived from inverse kinematic equation Eq. (8) is

$$\dot{X}(t) = P^{-1}(\theta)V(t). \quad (17)$$

The derivative of Eq. (17) with respect to time is

$$\ddot{X}(t) = \frac{\partial P^{-1}(\theta)}{\partial\theta}\dot{\theta}V(t) + P^{-1}(\theta)\dot{V}(t) \quad (18)$$

where

$$P^{-1}(\theta) = \begin{bmatrix} -\frac{2}{3}\sin\theta & -\frac{2}{3}\sin\left(\frac{\pi}{3}-\theta\right) & \frac{2}{3}\sin\left(\frac{\pi}{3}+\theta\right) \\ \frac{2}{3}\cos\theta & -\frac{2}{3}\cos\left(\frac{\pi}{3}-\theta\right) & -\frac{2}{3}\cos\left(\frac{\pi}{3}+\theta\right) \\ \frac{1}{3L} & \frac{1}{3L} & \frac{1}{3L} \end{bmatrix}$$

and

$$\frac{\partial P^{-1}(\theta)}{\partial\theta} = \begin{bmatrix} -\frac{2}{3}\cos\theta & \frac{2}{3}\cos\left(\frac{\pi}{3}-\theta\right) & \frac{2}{3}\cos\left(\frac{\pi}{3}+\theta\right) \\ -\frac{2}{3}\sin\theta & -\frac{2}{3}\sin\left(\frac{\pi}{3}-\theta\right) & \frac{2}{3}\sin\left(\frac{\pi}{3}+\theta\right) \\ 0 & 0 & 0 \end{bmatrix}.$$

The following theorem discloses the conditions of the vehicle dynamics simplified in a linear form.

Theorem 1: Let a three-wheel omnidirectional vehicle maneuver along a trajectory $X(t)$ in configuration space. If its wheels' velocities $V(t)$ related to $\dot{X}(t)$ satisfy inverse kinematic equation Eq. (8), then its dynamics (16) becomes

$$E\dot{V}(t) = (F\dot{\theta} + G)V(t) + \alpha U(t) + D(t) \quad (19)$$

where

$$E = \hat{P}^{-1}(\theta)\begin{bmatrix} m & 0 & 0 \\ 0 & m & 0 \\ 0 & 0 & J \end{bmatrix}P^{-1}(\theta) = \begin{bmatrix} \frac{4}{9}m + \frac{J}{9L^2} & -\frac{4}{9}m\cos\left(\frac{\pi}{3}\right) + \frac{J}{9L^2} & -\frac{4}{9}m\cos\left(\frac{\pi}{3}\right) + \frac{J}{9L^2} \\ -\frac{4}{9}m\cos\left(\frac{\pi}{3}\right) + \frac{J}{9L^2} & \frac{4}{9}m + \frac{J}{9L^2} & \frac{4}{9}m\cos\left(\frac{2\pi}{3}\right) + \frac{J}{9L^2} \\ -\frac{4}{9}m\cos\left(\frac{\pi}{3}\right) + \frac{J}{9L^2} & \frac{4}{9}m\cos\left(\frac{2\pi}{3}\right) + \frac{J}{9L^2} & \frac{4}{9}m + \frac{J}{9L^2} \end{bmatrix},$$

$$F = -\hat{P}^{-1}(\theta)\begin{bmatrix} m & 0 & 0 \\ 0 & m & 0 \\ 0 & 0 & J \end{bmatrix}\frac{\partial P^{-1}(\theta)}{\partial\theta} = -\begin{bmatrix} 0 & -\frac{4}{9}m\sin\left(\frac{\pi}{3}\right) & \frac{4}{9}m\sin\left(\frac{\pi}{3}\right) \\ \frac{4}{9}m\sin\left(\frac{\pi}{3}\right) & 0 & -\frac{4}{9}m\sin\left(\frac{2\pi}{3}\right) \\ -\frac{4}{9}m\sin\left(\frac{\pi}{3}\right) & \frac{4}{9}m\sin\left(\frac{2\pi}{3}\right) & 0 \end{bmatrix}, \text{ and}$$

$$G = -\hat{P}^{-1}(\theta)\begin{bmatrix} \frac{3\beta}{2} & 0 & 0 \\ 0 & \frac{3\beta}{2} & 0 \\ 0 & 0 & 3\beta L^2 \end{bmatrix}P^{-1}(\theta) = -\begin{bmatrix} \beta & -\frac{2}{3}\beta\cos\left(\frac{\pi}{3}\right) + \frac{\beta}{3} & -\frac{2}{3}\beta\cos\left(\frac{\pi}{3}\right) + \frac{\beta}{3} \\ -\frac{2}{3}\beta\cos\left(\frac{\pi}{3}\right) + \frac{\beta}{3} & \beta & \frac{2}{3}\beta\cos\left(\frac{2\pi}{3}\right) + \frac{\beta}{3} \\ -\frac{2}{3}\beta\cos\left(\frac{\pi}{3}\right) + \frac{\beta}{3} & \frac{2}{3}\beta\cos\left(\frac{2\pi}{3}\right) + \frac{\beta}{3} & \beta \end{bmatrix}.$$

Proof. Substituting Eqs. (17) and (18) into (19) results in

$$\begin{bmatrix} m & 0 & 0 \\ 0 & m & 0 \\ 0 & 0 & J \end{bmatrix}P^{-1}(\theta)\dot{V} = -\begin{bmatrix} m & 0 & 0 \\ 0 & m & 0 \\ 0 & 0 & J \end{bmatrix}\frac{\partial P^{-1}(\theta)}{\partial\theta}\dot{\theta}V - \begin{bmatrix} \frac{3\beta}{2} & 0 & 0 \\ 0 & \frac{3\beta}{2} & 0 \\ 0 & 0 & 3\beta L^2 \end{bmatrix}P^{-1}(\theta)V + \alpha\hat{P}(\theta)U(t) + \hat{P}(\theta)D(t) \quad (20)$$

After multiplying $\hat{P}^{-1}(\theta)$, Eq. (20) becomes

$$E\dot{V}(t) = (F\dot{\theta} + G)V(t) + \alpha U(t) + D(t).$$

□

If the vehicle is manipulated by fixed $\dot{\theta}$, the vehicle dynamics will be simplified to a linear time invariant system derived

https://doi.org/10.1017/S0263574709990890 Published online by Cambridge University Press

from Eq. (19)

$$\dot{V}(t) = AV + BU + E^{-1}D(t) \tag{21}$$

where $A = E^{-1}(F\Omega + G)$, $B = E^{-1}\alpha$, $\Omega = \dot{\theta}$ is a constant value, and $D(t)$ is the high-order disturbance produced by motor angular velocities. It is worthwhile to force $\dot{\theta}$ to a constant value Ω because the complicated dynamics of the omnidirectional vehicle can then be easily simplified to a linear system.

To summarize, there are two conditions to make the omnidirectional vehicle dynamics linear:

(1) Its kinematics Eq. (8), and
(2) Constant change in heading $\dot{\theta}(= \Omega)$.

Given a trajectory $\dot{X}(t)$ $([\dot{x}(t)\,])([\dot{x}(t)\,\dot{y}(t)\,\dot{\theta}(t)]^T)$, the three-wheel omnidirectional vehicle should been planned with Eq. (8) under condition (1) for its dynamics to be linear. Note that condition (2) does not restrict the position trajectory of the three-wheel omnidirectional vehicle. This is because the particular advantage of omnidirectional vehicles is that the orientation trajectory $\theta(t)$ is independent of the position trajectory $[x(t)\,y(t)]$. Hence, its orientation trajectory $\dot{\theta}(t)$ can be manipulated with regardless of its position trajectory $[\dot{x}(t)\ \dot{y}(t)]$. In general, it is not difficult to let the vehicle change by a fixed angle within the time of a fixed period. As a result, the three-wheel omnidirectional vehicle can be planned to maneuver on any position trajectory under condition (2). In Section 5, three kinds of trajectories illustrate how to keep its dynamics linear.

4. Design of a Linear Optimal Tracker

Once it is possible to linearize the dynamics of the three-wheel omnidirectional vehicle, linear optimal theories are suitable for its control. In this section, a linear optimal tracker for the control of the three-wheel omnidirectional vehicle is proposed. Finally, the linear optimal tracker is summarized by a calculation schema.

Let a linear time invariant system be Eq. (21), $W(t)$ be the desired velocity in which $t \in [t_0, T]$, and C be a linear combination matrix for the scalar of $v(t)$ corresponding to $W(t)$. Then, a controller $U(t)$ is designed for minimizing a performance index defined as follows:

$$J(t_0) = \frac{1}{2}Y(T)^T MY(T) + \frac{1}{2}\int_{t_0}^{T} [Y(t)^T QY(t) + U(t)^T RU(t)]\mathrm{d}t, \tag{22}$$

where $Y(t) = (CV(t) - W(t))$ is the tracking error of wheel velocity, M, Q, and R are the matrices of weighting factors for terminal condition, tracking error and controller output, respectively, and $M \geq 0$, $Q \geq 0$, and $R > 0$ are all symmetric. Note that $D(t)$, the high-order variables in Eq. (21), is regarded as system disturbance. Therefore, the control problem of the vehicle based on this performance index becomes optimal tracking control with disturbance.

Here, a linear optimal tracking controller based on continuous linear quadratic tracker[18] is designed. However, the system as shown in Eq. (21) includes disturbance $D(t)$ that is temporarily neglected. The linear optimal tracking control law for the system with disturbance should be solved as follows:

Theorem 2: For the linear time invariant dynamic system Eq. (21), the linear optimal tracker designed for the performance index Eq. (22) is,

$$-\dot{S} = A^T S + SA - SBR^{-1}B^T S + C^T QC, \quad S(T) = C^T MC, \tag{23}$$

$$K(t) = R^{-1}B^T S(t), \tag{24}$$

$$-\dot{g} = (A - BK)^T g + C^T QW - SE^{-1}D, \quad g(T) = C^T MW(T) \tag{25}$$

$$U(t) = -K(t)V(t) + R^{-1}B^T g(t) \tag{26}$$

where Eq. (23) is a matrix Riccati equation for $S(t)$ with final condition $S(T)$, $K(t)$ is the gain matrix, Eq. (25) is an auxiliary differential equation for $g(t)$ with final condition $g(T)$, and $U(t)$ is the controller output of the optimal tracker.

Proof. Define a Hamiltonian equation by combining Eqs. (21) and (22)

$$H(V, u, t) = \frac{1}{2}[(CV - W)^T Q(CV - W) + U^T RU] + \lambda^T(AV + BU + E^{-1}D). \tag{27}$$

A state equation and a costate equation are obtained by

$$\dot{V} = \frac{\partial H}{\partial \lambda} = AV + BU + E^{-1}D, \text{ and} \tag{28}$$

$$-\dot{\lambda} = \frac{\partial H}{\partial V} = A^T\lambda + C^T QCV - C^T QW, \text{ respectively.} \tag{29}$$

From stationary condition, we have

$$U = -R^{-1}B^T\lambda \tag{30}$$

Let the costate be

$$\lambda = SV - g(t) \tag{31}$$

where S is the solution of Eq. (23), and $g(t)$ is driven by reference $W(t)$. Hence, the derivative of Eq. (31) with respect to time is

$$\dot{\lambda} = \dot{S}V + S\dot{V} - \dot{g}. \tag{32}$$

Combining Eqs. (23), (29), (31) and (32) together results in

$$-\dot{S}V + \dot{g} = A^T SV - A^T g + SAV + SBU + SE^{-1}D + C^T QCV - C^T QW. \tag{33}$$

Moreover, substituting Eq. (31) into (30) results in

$$U = -R^{-1}B^T SV + R^{-1}B^T g. \tag{34}$$

https://doi.org/10.1017/S0263574709990890 Published online by Cambridge University Press

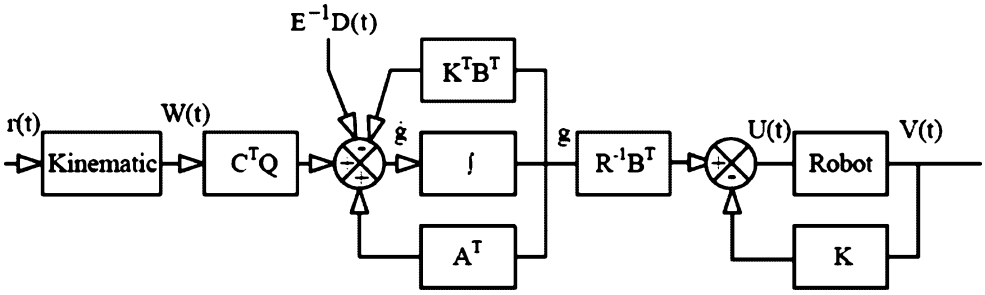

Fig. 3. The calculation schema of the linear optimal tracker for overcoming disturbance.

Substituting Eq. (34) into Eq. (33) obtains

$$-\dot{S}V + \dot{g} = A^T SV - A^T g + SAV - SBR^{-1}B^T SV + SBR^{-1}B^T g + SE^{-1}D + C^T QCV - C^T QW. \tag{35}$$

Let

$$-\dot{S} = A^T S + SA - SBR^{-1}B^T S + C^T QC, \text{ and } K(t) = R^{-1}B^T S(t). \tag{36}$$

Then, Eq. (35) can be simplified to

$$-\dot{g} = (A - BK)^T g + C^T QW - SE^{-1}D. \tag{37}$$

Eqs. (34), (36) and (37) are the control law of the linear optimal tracker for the system with known disturbance. □

To summarize, the linear optimal tracker consists of an optimal tracking controller and a kinematic transformation to achieve the mission that the wheels' velocity trajectories satisfy its kinematic constraint. Figure 3 schematizes the linear optimal tracker. The goal of the linear optimal tracker is to control wheel velocities $V(t)$ to track $W(t)$ which is transformed from $r(t)$ based on the vehicle kinematics. There are two closed loops in Fig. 3. The first closed loop calculates the auxiliary function $g(t)$ for tracking $W(t)$ and rejecting the disturbance $E^{-1}D(t)$. After obtaining $g(t)$, the linear optimal controller $U(t)$ is calculated to control the vehicle in the second closed loop. Notice that the calculation of the gain matrix $K(t)$ is not shown in Fig. 3. $K(t)$ is obtained from Eq. (24) after solving $S(t)$ from the Riccati Eq. (23). In addition, the integration interval of Eqs. (23) and (25) should be replaced by $[T, 0]$ after canceling the minus signs of their left-hand sides because their boundary conditions given are the terminal values $S(T) = C^T MC$ and $g(T) = C^T MW(T)$, respectively. Therefore, if the tracked signal $W(t)$ and the disturbance $E^{-1}D(t)$ are given, $K(t)$ and $g(t)$ are stored by off-line computation. When the vehicle motors are controlled by the control signal $U(t)$ calculated from $K(t)$ and $g(t)$, $V(t)$ tracks $W(t)$.

5. Trajectory Planning for Kinematic Constraints

When designing a vehicle movement trajectory, it is essential to carefully plan wheel velocities to satisfy the conditions that the vehicle dynamics is linear. In this section, three cases, each with a different kind of trajectories, illustrate the planning strategy.

Let $r(t) = [r_x(t)\, r_y(t)\, r_\theta(t)]^T \in X(t)$ be the vehicle movement trajectory in configuration space based on workspace (x_b, y_b), and $W(t) = [w_1(t)\, w_2(t)\, w_3(t)]^T \in V(t)$ be the desired wheel velocity trajectory. Under the second condition, $\dot{r}_\theta(t)$ must be constant when planning wheels' velocities $W(t)$ for the vehicle movement trajectory. As well, it is necessary to design $W(t)$ to satisfy inverse kinematics Eq. (8):

$$W(t) = P(\theta)\dot{r}(t) = P(\theta)\left[\dot{r}_x(t)\ \dot{r}_y(t)\ \dot{r}_\theta(t)\right]^T. \tag{38}$$

where $\dot{r}_x(t) = \frac{\partial r_x(t)}{\partial t}$, $\dot{r}_y(t) = \frac{\partial r_y(t)}{\partial t}$, and $\dot{r}_\theta(t) = \frac{\partial r_\theta(t)}{\partial t}$. Given trajectories $r(t)$, the objective of trajectory planning is finding the wheel velocity trajectories $W(t)$.

It is well known that continuity is an important consideration in trajectory planning. Here, the vehicle velocity is designed to be piecewise continuous. Let $|r(t)|$ be the maneuver distance of the vehicle, and $v_{\text{vehicle}}(|r(t)|)$ be the vehicle movement velocity. Figure 4 is the profile of the vehicle velocity planned for piecewise continuity, where $|r_d(t)|$ is the destination distance. In Fig. 4, the horizontal line also represents time. The time periods separated by t_1, t_2 and t_3 are the regions of acceleration, constant velocity and deceleration, respectively. Planning only considers trajectories, which begin with acceleration and end with and deceleration, giving a piecewise-continuous velocity. Consequently, when planning a trajectory $r(t)$, the vehicle movement velocity trajectory $v_{\text{vehicle}}(|r(t)|)$ gives us the vehicle movement velocity $\dot{r}(t)$. After solving $\dot{r}(t)$, wheel velocity trajectories $W(t)$ can be calculated by Eq. (38).

Planning of the vehicle velocity trajectory as shown in Fig. 4 allows us to alleviate the disturbance of the un-modeled high-order term, $d(\omega)$. In most of vehicle trajectories, the

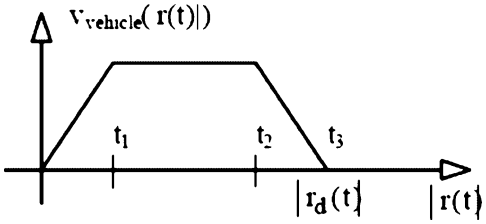

Fig. 4. The profile of planning vehicle velocity.

https://doi.org/10.1017/S0263574709990890 Published online by Cambridge University Press

wheel angle jerk ($\ddot{\omega}$) is zero on this kind of velocity trajectory. The wheel angle acceleration ($\dot{\omega}$) is zero in the time period (t_1, t_2). Consequently, the vehicle velocity trajectory planning only has a disturbance $d(\omega)$ resulted from the wheel angle acceleration and deceleration in time periods (0, t_1) and (t_2, t_3).

It is crucial to solve $W(t)$ to satisfy Eq. (38) at the initial conditions of trajectory planning. In general cases, the velocity profile as shown in Fig. 4 supposes that the vehicle movement begins from rest, i.e. $W(0) = [0\,0\,0]^T$. At each sampling period, we calculate Eq. (38) for $W(t)$ so that the whole trajectory satisfies the vehicle kinematic equation. However, the initial velocities of the three wheels may not be zero in special cases such as a trajectory consisting of two intersecting straight lines. It is difficult to still satisfy Eq. (38) when the wheel velocities change from the first line to the second lines. To illustrate trajectory planning in detail, we discuss three cases: a straight line, a circle and two intersecting lines.

Case 1: A straight line

Let the angle between the straight line of the vehicle movement and X_b (horizontal line) be θ_d. θ_d is a constant for the straight line. The straight line, therefore, satisfies

$$\dot{r}_x(t) = v_{\text{vehicle}}(|r(t)|)\sin(\theta_{\text{d}}),$$
$$\dot{r}_y(t) = v_{\text{vehicle}}(|r(t)|)\sin(\theta_{\text{d}}),$$

and

$$\dot{r}_\theta(t) = 0 \tag{39}$$

where $v_{\text{vehicle}}(|r(t)|)$ is the trajectory as shown in Fig. 4. For the straight line, $w_1(t)$, $w_2(t)$ and $w_3(t)$ are solved by substituting Eq. (39) into Eq. (38). Notice that $\dot{r}_\theta(t) = 0$ satisfies the first condition of linear vehicle dynamics, and that in a nonholonomic vehicle (or mobile robot), r_θ must equal θ_d, but omnidirectional vehicles don't have this constraint. Simulation in the next section will show this property.

Case 2: A circle trace

Let r_R be the radius of a circle trace. Then, the relationship between the linear velocity and the angular velocity of the vehicle (see Eq. (13)) is obtained by

$$\dot{r}_\theta(t) = \frac{v_{\text{vehicle}}(|r(t)|)}{r_R}. \tag{40}$$

The equation of the circle is

$$r_x(t) = r_R \sin(r_\theta(t)), \text{ and}$$
$$r_y(t) = r_R \sin(r_\theta(t)). \tag{41}$$

The derivative of Eq. (41) with respect to time is

$$\dot{r}_x(t) = -r_R \sin(r_\theta(t))\dot{r}_\theta(t), \text{ and}$$
$$\dot{r}_y(t) = r_R \cos(r_\theta(t))\dot{r}_\theta(t). \tag{42}$$

Eqs. (40) and (42) substituted into Eq. (38) can solve $w_1(t)$, $w_2(t)$ and $w_3(t)$ for the wheels' velocity trajectories. Two situations, fixed $\dot{r}_\theta(t)$ and r_θ (i.e. $\dot{r}_\theta(t) = 0$), meet the second conditions of the vehicle in linear dynamics. Simulation in the next section will show both situations.

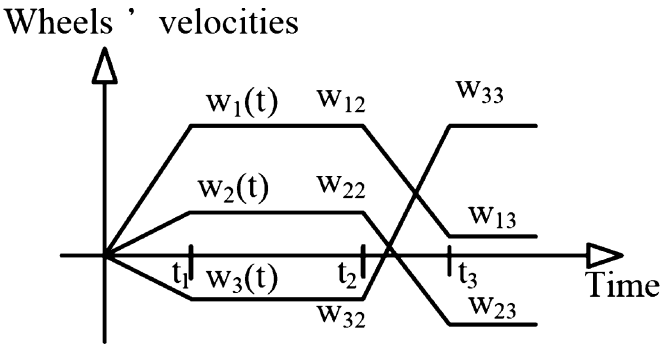

Fig. 5. The velocity profile during the change of wheel velocities.

Case 3: Two intersecting lines

In this case, the key point of trajectory planning is the change in wheel velocities from the end of the first straight line to the beginning of the second one. It is difficult during this period to always satisfy kinematic Eq. (8). The trajectory planning of this case is illustrated by an example below.

In Fig. 5, the time $[0, t_2]$ shows the vehicle as it moves along the first straight line. The wheel velocity vector at t_2 is $[w_{1,2}, w_{2,2}, w_{3,2}]$. The vehicle steered by wheel velocity vector $[w_{1,3}, w_{2,3}, w_{3,3}]$ follows the second straight line beginning at time t_3. If the wheel velocity vector is $[w_{1,3}, w_{2,3}, w_{3,3}]$ at t_3, it is not difficult to steer the vehicle on the second straight line after t_3. During the time interval $[t_2, t_3]$, the wheel velocity vector needs to change from $[w_{1,2}, w_{2,2}, w_{3,2}]$ to $[w_{1,3}, w_{2,3}, w_{3,3}]$ so that the vehicle movement can change from the first straight line to the second straight line.

The strategy makes use of the maximum change velocity as its basis. As shown in Fig. 5, the velocity of maximum change is

$$a_3 = \max_{i=1,\ldots 3} \left| w_{i,j+1} - w_{i,j} \right| = w_{3,3} - w_{2,3}. \tag{43}$$

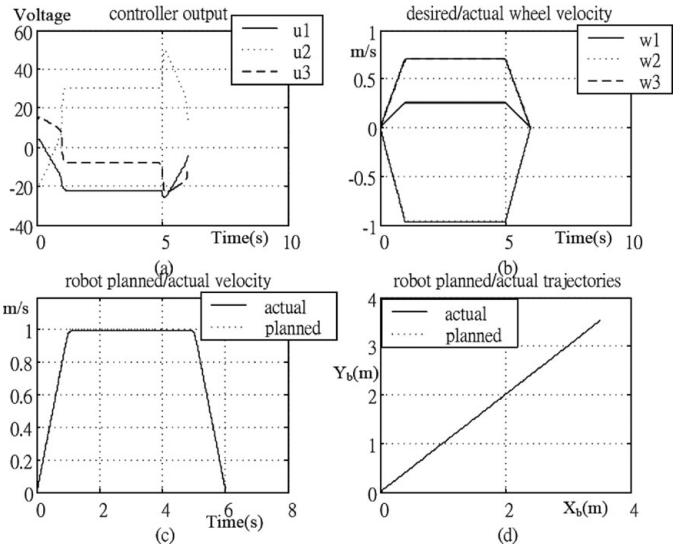

Fig. 6. The linear optimal tracker for the omnidirectional vehicle with disturbance.

https://doi.org/10.1017/S0263574709990890 Published online by Cambridge University Press

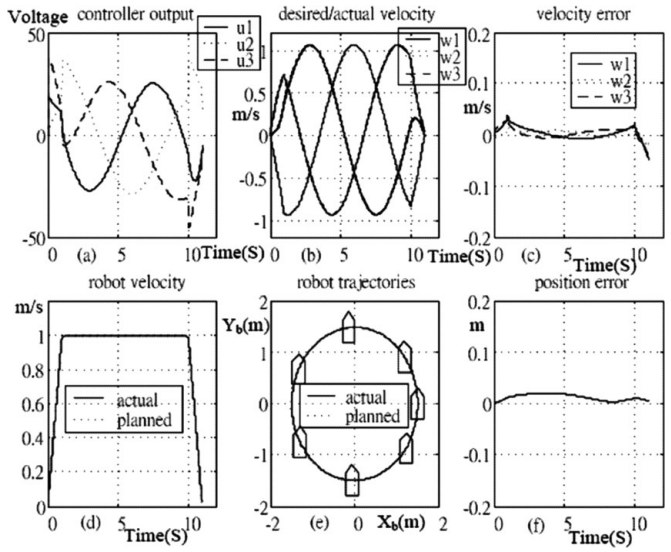

Fig. 7. The linear optimal tracker for tracking a circle trajectory.

where $w_{i,j}$ is ith wheel velocity at time t_j. Hence, a_3 is selected as the basis of velocity change. Let the maximum motor acceleration be a_m. Then the time of velocity change is designed by

$$t_p = \frac{a_3}{a_m} \tag{44}$$

The acceleration of the other wheels is designed according to t_p. This strategy is thus to vary acceleration (or deceleration) within a fixed period. The acceleration of wheels 1 and 2 is

$$a_1 = \frac{(w_{1,j+1} - w_{1,j})}{t_p}, \text{ and}$$
$$a_2 = \frac{(w_{2,j+1} - w_{2,j})}{t_p}, \text{ respectively.} \tag{45}$$

where $w_{1,j}$ is the velocity of wheel 1 at time t_j, and $w_{2,j}$ is that of wheel 2 at t_j. Note that wheel 3 uses the maximum acceleration, i.e., $a_3 = a_m$. The trajectory planning of the three cases is demonstrated by simulation in next section.

6. Simulation and Experiments

In this section, the linear optimal tracker is implemented by simulation and experiments. Simulation includes three kinds of trajectories discussed in the previous section.

In the study, the motor is a model 1524 made of Faulhaber group (http://www.faulhaber-group.com/). When the linear optimal tracker design includes disturbance $D(t)$, Fig. 6 shows that the omnidirectional vehicle follows the planned trajectory very well. Notice that the simulation fixes the vehicle orientation at $\pi/6$ (i.e. $r_\theta = \pi/6$).

Figures 7 and 8 show the vehicle controlled to follow a circle trace in different orientations. In Fig. 7, the vehicle orientation is fixed at $\pi/2$, but in Fig. 8 its orientation follows the circle trace, i.e. $\dot{r}_\theta$ is fixed. In addition to trajectory tracking, the sub-figures (e) of Figs. 7 and 8 show the vehicle's instantaneous orientation. Both results show that the optimal controller does a good job tracking the desired trajectories for constant r_θ and $\dot{r}_\theta$. Sub-figures (c) and (f)

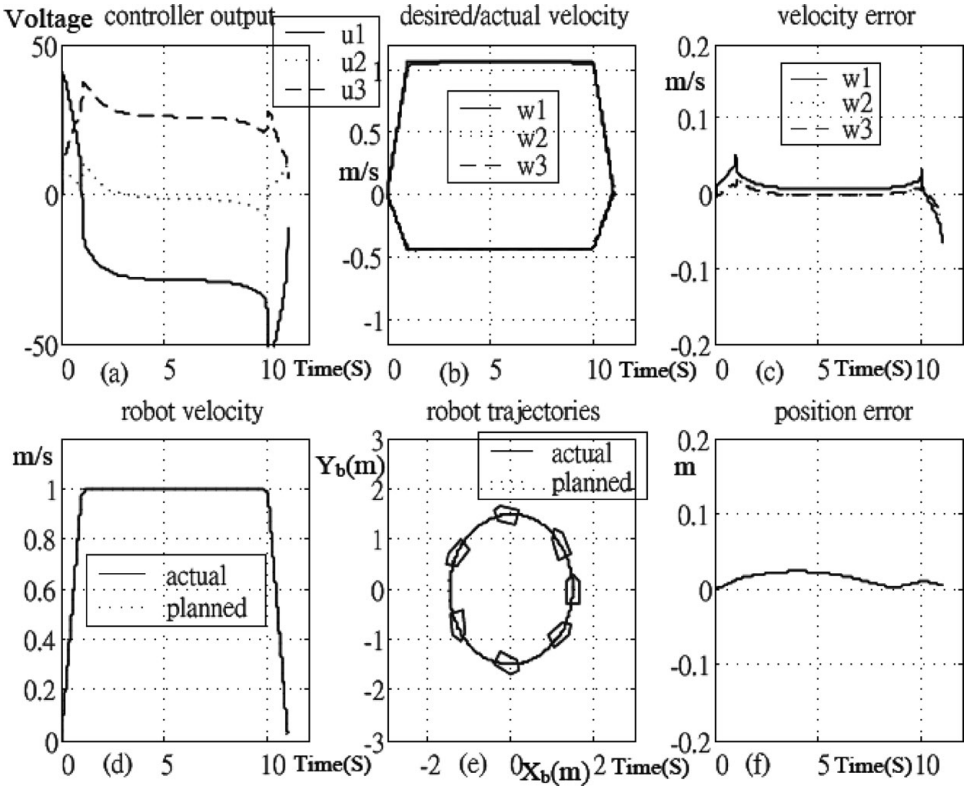

Fig. 8. The linear optimal tracker for tracking a circle trajectory.

https://doi.org/10.1017/S0263574709990890 Published online by Cambridge University Press

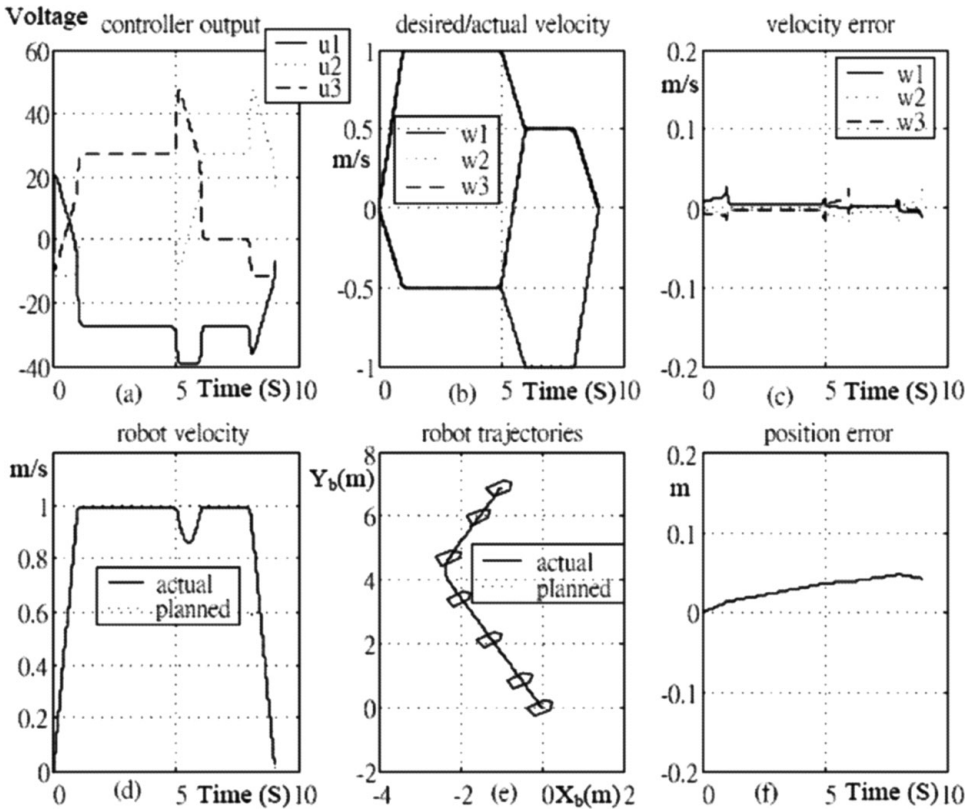

Fig. 9. The linear optimal tracker for tracking two straight lines at different slopes.

show the tracking errors of wheel velocities and vehicle position, respectively.

Simulation includes controlling the vehicle to follow two connected straight lines of different slopes. Figure 9(e) shows that the vehicle can be controlled at orientation $\pi/6$ to follow the two straight lines very well. Sub-figures (c) and (f) show the trajectory errors of wheels' velocities and the vehicle position, respectively.

In this study, a real omnidirectional vehicle was implemented for experiments. Figure 10 is the vehicle viewed from the top and bottom. In the vehicle, a radio frequency module is installed to receive experimental command, and a RS-232 cable is connected to a personal computer for storing experimental data. There are two experiments: one to control the vehicle to track a straight line, the other to track a circle.

Zero slip, an assumption in the derivation of the omnidirectional mobile vehicle dynamic model, must be carefully maintained during practical experiments. Wheel slip arises from too much acceleration. Therefore, we performed an experiment to find the maximum slip-free acceleration, by controlling the vehicle over a fixed distance. When the vehicle wheels cause slip, the motor's encoder still counts wheel movement but without corresponding vehicle movement. Wheel slip can thus be identified if the vehicle moves less than the defined distance. After many tests, we found out that the maximum slip-free acceleration on carpet was about 0.8 m/s^2, as shown in Fig. 10.

In the experiments, sampling interval is 1 ms (millisecond), and motors' positions in each sampling interval was stored to estimate velocity. Too high a desired velocity makes

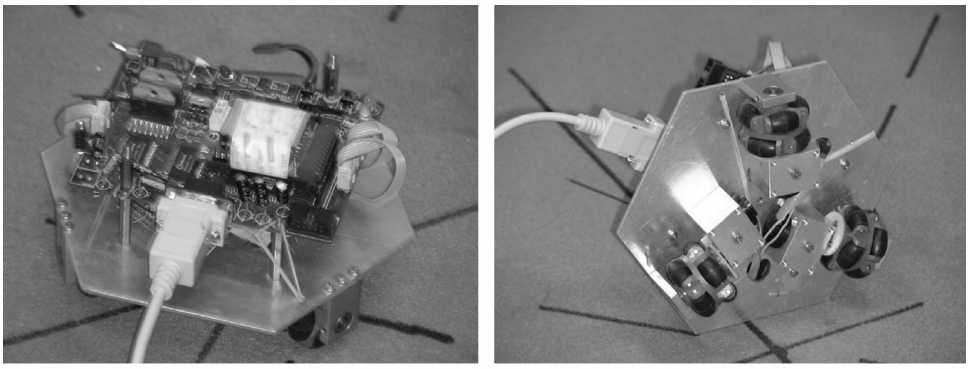

(a) top view (b) bottom view

Fig. 10. The photo of the omnidirectional mobile vehicle.

https://doi.org/10.1017/S0263574709990890 Published online by Cambridge University Press

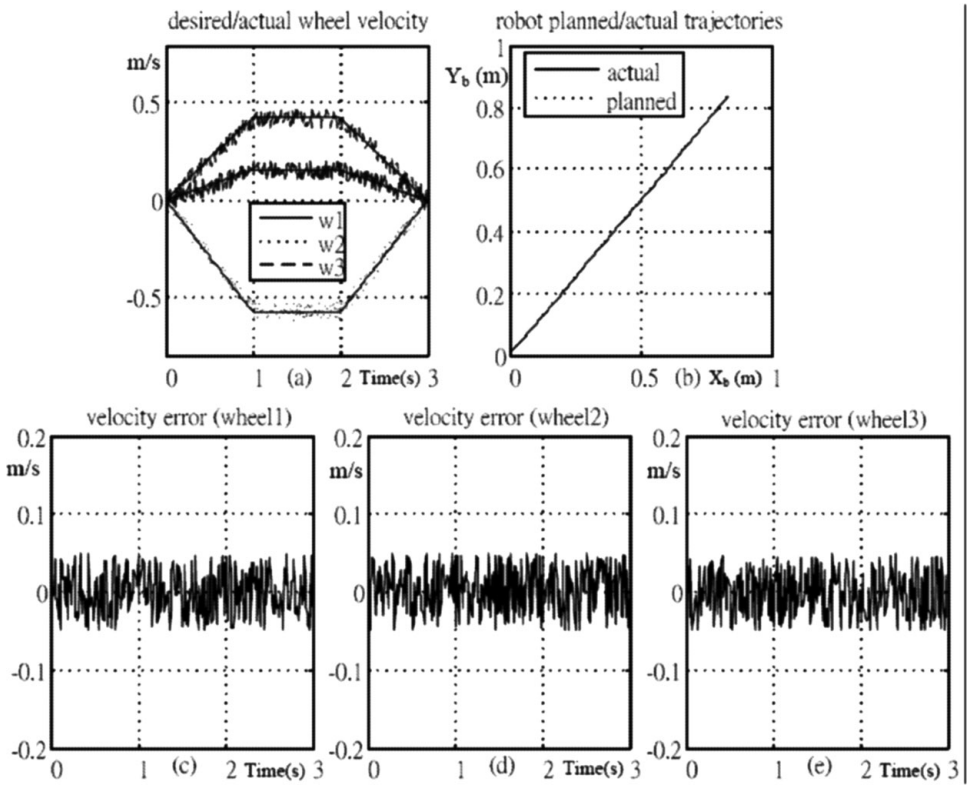

Fig. 11. The wheels' velocities and tracking errors of the real vehicle controlled to follow a straight line.

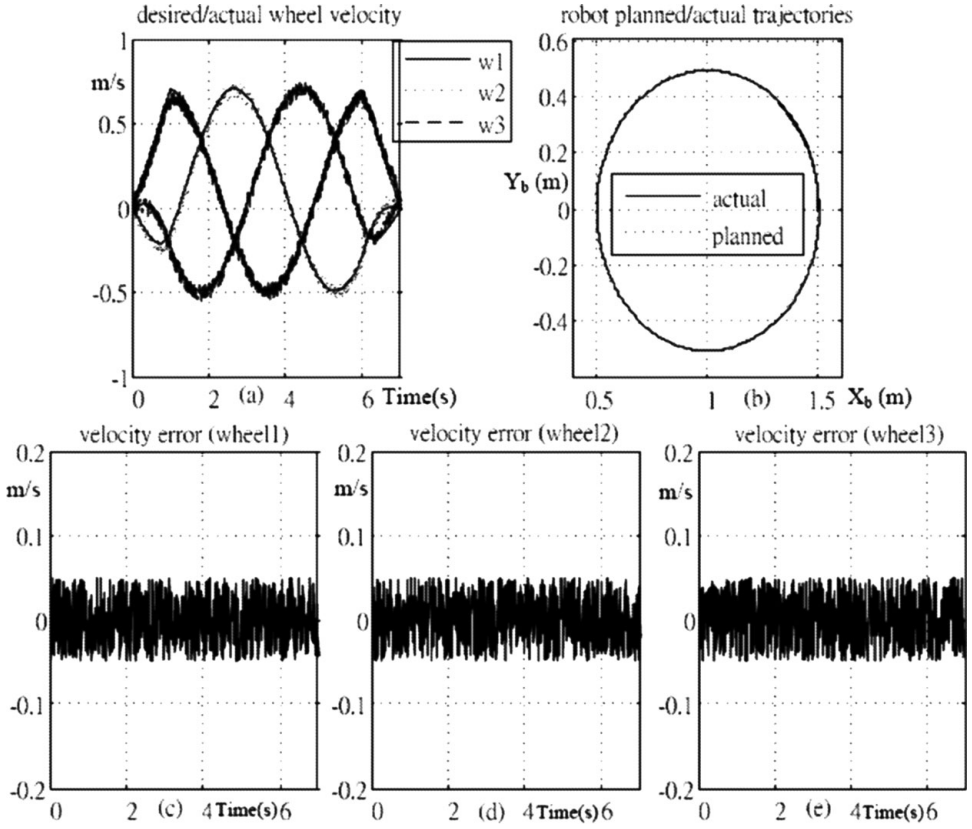

Fig. 12. The wheels' velocities and tracking errors of the real vehicle controlled to follow a circle.

https://doi.org/10.1017/S0263574709990890 Published online by Cambridge University Press

wheel velocity tracking difficult, because limited battery energy means that the vehicle cannot attain arbitrarily high velocities. By experimentation, we found that the wheel velocities could be tracked very well if the vehicle moved under velocity 0.6 m/s. Figures 11 and 12 show the results of wheel velocities and tracking errors as the vehicle follows a straight line and a circle, respectively.

7. Conclusions and Further Developments

An omnidirectional vehicle has its intrinsic motion characteristics: the kinematic relationship between its body movement and wheels' rotation velocities. In this paper, kinematics makes the dynamics of an omnidirectional vehicle linear when its orientation change rate is fixed (i.e. constant $\dot{\theta}$). Hence, the difficult control problem of omnidirectional vehicles can be resolved by classical control theories. It is interesting but not surprising that the vehicle's dynamics is related to its kinematics. Our research demonstrates that complicated dynamics solved by kinematics is an easy way to control omnidirectional vehicles. In addition, the examples of planning wheel trajectory for maintaining the conditions of the vehicle dynamics in linear illustrate that the vehicle movement trajectories of straight lines and circle traces are easy, but those of two straight lines with different slopes are difficult. However, the strategy of varying acceleration in a fixed period solves the difficulty of the latter case. Simulation and experiments demonstrate these study results.

In this paper, motion planning makes the omnidirectional vehicle linear, like decoupling the interaction among its three wheels. In contrast to conventional motion planning, which usually focuses on smooth trajectories, this is innovative, and a concrete improvement on this control problem. In general, controller design of robots only takes care of its dynamics, but ignores its kinematics. This methodology paves a way to consider kinematics and dynamics together for controlling robots simply and easily. This suggests further development to study controller design of robot arms, legs, and so on.

Acknowledgments

This research was supported by National Science Council, Taiwan, Rep. of China under Grants NSC-92-2213-E-327-013.

References

1. R. Balakrishna and A. Ghosal, "Modeling of slip for wheeled mobile robots," *IEEE Trans. Robot. Autom.* **11**(1), 126–132 (1995).
2. A. Bétourné and G. Campion, "Dynamic Modeling and Control Design of a Class of Omnidirectional Mobile Robots," *IEEE Int. Conf. on Robotics and Automation* (1996) pp. 2810–2815.
3. J. Borenstein, H. R. Everett and L. Feng, "Mobile robot positioning: Sensors and techniques," *J. Robot. Syst.* **14**, 231–249 (1997).
4. C. Canudas de Wit, "Trends in mobile robot and vehicle control," *Control Problems in Robotics and Automation* 151–175 (1998).
5. R. D'Andrea, T. Kalmár-Nagy, P. Ganguly and M. Babish, "The Cornell RoboCup Team," **In**: *Robot Soccer World Cup IV, Lecture Notes in Artificial Intelligence* (G. Kraetzschmar, P. Stone and T. Balch, eds.) vol. 2019, (Springer, Berlin, 2001), pp. 41–51.
6. B. D'Andréa-Novel, G. Bastin and Campion, "Modelling and Control of Non Holonomic Wheeled Mobile Robots," *IEEE Int. Conf. on Robotics and Automation* (1991) pp. 1130–1135.
7. N. Faiz and S. K. Agrawal, "Trajectory Planning of Robots with Dynamics and Inequalities," *IEEE Int. Conf. on Robotics and Automation* (2000) pp. 3976–3982.
8. L. Ferrière, G. Campion and B. Raucent, "POLLMOBS, a new drive system for omnimobile robots," *Robotica* **19**, 1–9 (2001).
9. R. Fierro and F. L. Lewis, "Control of a nonholonomic mobile robot: backstepping kinematics into dynamics," *J. Robot. Syst.* **14**(3), 149–163 (1997).
10. T. Fraichard and A. Scheuer, "From Reeds and Shepp's to continuous-curvature paths," *IEEE Trans. Robot. Autom.* **20**, 1025–1035 (2004).
11. E. Frazzoli, M. A. Dahleh and E. Feron, "Real-time motion planning for agile autonomous vehicles," *J. Guid. Control Dyn.* **25**(1), 116–129 (2001).
12. T. Fukao, H. Nakagawa and N. Adachi, "Adaptive tracking control of a nonholonomic mobile robot," *IEEE Trans. Robot. Autom.* **16**(5), 609–615 (2000).
13. L. Gracia and J. Tornero, "A new geometric approach to characterize the singularity of wheeled mobile robots," *Robotica* **25**, 627–638 (2007).
14. L. Gracia and J. Tornero, "Kinematic models and isotropy analysis of wheeled mobile robots," *Robotica* **26**, 587–599 (2008).
15. H. C. Huang and C. C. Tsai, "Simultaneous tracking and stabilization of an omnidirectional mobile robot in polar coordinates: a unified control approach," *Robotica* **27**, 1–12 (2008).
16. Z.-P. Jiang and H. Nijmeijer, "Tracking control of mobile robots: a case study in backstepping," *Automatica* **33**(7), 1393–1399 (1997).
17. T. Kalmár-Nagy, R. D'Andrea and P. Ganguly, "Near-optimal dynamic trajectory generation and control of an omnidirectional vehicle," *Robot. Auton. Syst.* **46**, 47–64 (2004).
18. F. L. Lewis and V. L. Syrmos, *Optimal Control*, ch. 42nd ed. (J. Wiley & Sons, 1995), Canada.
19. Z. Li, J. Chen and J. Feng, "Design of an omni-directional mobile microrobot (OMMR-I) for a micro-factory with 2 mm electromagnetic micromotors," *Robotica* **23**, 45–49 (2005).
20. K. L. Moore and N. S. Flann,, "A six-wheeled omnidirectional autonomous mobile robot," *IEEE Control Syst. Mag.* **20**(6), 53–66 (2000).
21. V. Muñoz, A. Ollero, M. Prado and A. Simón, "Mobile robot trajectory planning with dynamic and kinematic constraints," *Proc. of the IEEE Intern. Conf. on Robotics and Autom.* **4**, 2802–2807 (1994).
22. F. G. Pin and S. M. Killough, "A new family of omnidirectional and holonomic wheeled platforms for mobile robot," *IEEE Trans. Robot. Autom.* **19**(4), 480–489 (1994).
23. O. Purwin and R. D'Andrea, "Trajectory Generation for Four Wheeled Omnidirectional Vehicles," *Proceedings of American Control Conf.* (2005) pp. 4979–4984.
24. P.-S. Tsai, L.-S. Wang, F.-R. Chang and T.-F. Wu, "Systematic Backstepping Design for B-Spline Trajectory Tracking Control of the Mobile Robot in Hierarchical Model," *Proceedings of IEEE Int. Conf. on Networking, Sensing and Control* (2004) pp. 713–718.
25. R. L. Williams, II, B. E. Carter, P. Gallina and G. Rosati, "Dynamic model with slip for wheeled omnidirectional robots," *IEEE Trans. Robot. Autom.* **18**(3), 185–293 (2002).